

International Journal of Nanoelectronics and Materials

IJNeaM

ISSN 1985-5761 | E-ISSN 2232-1535



Design and simulation of a high-sensitivity MEMS capacitive pressure sensor

Illiana Khalida Mohd Shukri a , Hasnizah Aris a,b *, Nurul Izza Mohd Nor a,b , Mohd Hafiz Ismail a , Nazuhusna Khalid a,b , Wan Mokhdzani Wan Norhaimi a , Zaliman Sauli a,b , and Anees Abdul Aziz c

^aFaculty of Electronic Engineering & Technology, Universiti Malaysia Perlis (UniMAP), 02600 Arau, Perlis, Malaysia ^bCentre of Excellence for Micro System Technology (MiCTEC), Universiti Malaysia Perlis (UniMAP), 02600 Arau, Perlis, Malaysia ^cIntegrated Microelectronic System and Application Research Group, School of Electrical Engineering, College of Engineering, Universiti Teknologi MARA, 40450 Shah Alam, Selangor, Malaysia

* Corresponding author. Tel.: +6019-7764486; e-mail: hasnizah@unimap.edu.my

Received 19 December 2024, Revised 04 September 2025, Accepted 01 October 2025

ABSTRACT

A MEMS capacitive pressure sensor is a device used to measure changes in capacitance resulting from pressure-induced deformations in a diaphragm. In this paper, the designed sensor was simulated using Finite Element Analysis (FEA) simulation tools, which began with the visualisation of the layout using Blueprint. Then, by utilising the IntelliFab, the fabrication processes are defined, and subsequently, the 3D model of the sensor is generated in FabSim. The 3D model has gone through the preprocessing steps that included boundary conditions setup, materials properties setting, and loads application on the sensor's diaphragm. The first MEMS capacitive pressure sensor design uses a square-shaped Si diaphragm with dimensions of 150 μ m × 150 μ m and a thickness of 1 μ m. It is separated by a 2 μ m air gap and sandwiched between two Mo electrodes, each 1 μ m thick. This design achieves a resonance frequency of 947.702 kHz, with a maximum Z-displacement of 7.88×10-17 μ m under a static pressure of 20 MPa. At an applied pressure of 1 MPa, the maximum capacitance value reaches 95.89 fF. The overall sensitivity of this design is 31.861 fF/MPa. The second design incorporates 200 μ m-long beams attached to the square-shaped Si diaphragm. This configuration achieves a resonance frequency of 13.526 kHz, with a maximum Z-displacement of 0.244 μ m under a static pressure of 20 MPa. At an applied pressure of 4 × 10-4 MPa, the maximum capacitance value reaches 1.129 pF. The sensitivity of this design is 2.505 × 106 fF/MPa.

Keywords: Capacitive pressure sensor, FEA, High sensitivity

1. INTRODUCTION

A Micro-Electro-Mechanical System (MEMS) pressure sensor is a fundamental component in various systems. They are electronic devices that serve the purpose of detecting the pressure level of an element. MEMS Pressure sensor applications are expanding rapidly because of technological advancements, creating a wide range of demands in various industries, including medical, automotive, industrial, and aerospace, due to multiple benefits such as compact size, lightweight design, high-pressure sensitivity, and compatibility. Pressure sensors can be categorized in various ways, including the type of pressure measurement, application, or sensing elements, such as piezoelectric, capacitive, and piezoresistive pressure sensors [1, 2].

A piezoelectric sensor is a device that measures the change in pressure, strain, or force and converts it to an electronic signal by utilizing the piezoelectric effect to detect applied mechanical stress. The phenomenon referred to as the piezoelectric effect occurs when specific materials undergo mechanical stress and produce an electric charge [3].

Capacitive pressure sensors consist of two plates, called top and bottom electrodes, with an air gap or dielectric between

them. The bottom electrode is fixed, and pressure is applied on top of the upper diaphragm, which deforms it, changing the electrode gap. This effective gap change affects the capacitance between two electrodes [4].

The piezoresistivity pressure sensor operates on the mechanical deformation and stress of pressure on thin diaphragms. The piezoresistors transform the diaphragm stress caused by applied pressure into a change in electrical resistance, which is converted into voltage output using a Wheatstone bridge circuit [5].

Among all the MEMS pressure sensor transduction principles, piezoresistive and capacitive transduction mechanisms have been widely used. The disadvantage of employing piezoelectric material is that its performance is substantially affected by temperature [6]. While piezoelectric sensors are significantly influenced by temperature variations that affect their performance, piezoresistive sensors require complex temperature compensation and generally consume more power, which can be prohibitive for battery-powered and wearable devices. Consequently, MEMS capacitive pressure sensors have gained prominence due to their superior sensitivity, low power consumption, temperature stability, and ease of integration with semiconductor processes [7–9].

Despite extensive research and technological advancement in MEMS capacitive pressure sensors, there is still a need for enhancing their sensitivity to satisfy the higher precision and robustness requirements [10]. Researchers have explored various strategies, including material innovations, structural modifications, and novel diaphragm designs, to amplify sensitivity. Recent studies suggest that integrating beam structures with the diaphragm can effectively increase deflection and sensitivity; however, there is a limited scope of systematic investigation into optimizing beam geometry to maximize sensor performance without compromising mechanical stability or fabrication feasibility [9, 11].

This research addresses this gap by focusing on the optimization of the beam geometry attached to the diaphragm in MEMS capacitive pressure sensors. The goal is to achieve enhanced sensitivity suitable for applications demanding high accuracy, while maintaining low power consumption and operational stability under varying environmental conditions. This approach aims to contribute a meaningful advance to the design and practical implementation of MEMS capacitive pressure sensors.

2. THEORETICAL OF MEMS CAPACITIVE PRESSURE SENSOR DESIGN

In MEMS, a basic capacitive sensor consists of two parallel plates: a thin, flexible conductive membrane (diaphragm) and a permanent back plate separated by a small air gap. When an external force, such as pressure or acceleration, is applied, the diaphragm deflects, causing a change in the air gap which affects the capacitance of the sensor. The capacitive pressure sensor can be square, rectangular, circular, hexagonal, or any other shape, and the diaphragm shape can be arbitrarily [12]. Figure 1 shows the pressure sensor's schematic 2-dimensional (2D) illustration. This pressure sensor has utilized graphene as the membrane, with the air functioning as the dielectric.

Theoretically, the structure of a parallel-plate MEMS capacitive sensor can be depicted in Figure 2. Two parallel conductive plates have an overlapped area, denoted as *A*, and are separated by a dielectric with a distance of *d*.

The value of the capacitance, *C*, between the two plates is defined as in Equation (1):

$$C=Q/V$$
 (1)

where Q is the amount of stored charge and V is the electrostatic potential. The electric energy stored by a given capacitor, U, is expressed as Equation (2):

$$U = \frac{1}{2}CV^2 = \frac{1}{2}\frac{Q^2}{C} \tag{2}$$

For a parallel-plate capacitor, electric field lines are parallel to each other and perpendicular to the plate surfaces in the overlapped region. According to Gauss's law, the magnitude of the primary electric field, E, is related to Q by Equation (3):

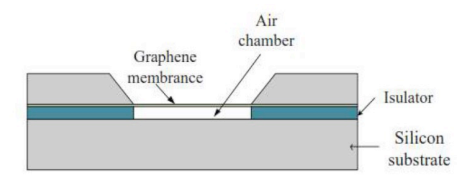


Figure 1. Cross-section view of 2D MEMS capacitive pressure sensor [12]

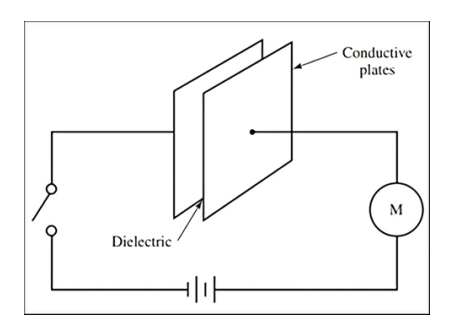


Figure 2. Basic form of a capacitor

$$E = \frac{Q}{\varepsilon A} \tag{3}$$

The magnitude of the voltage is the electric field times the distance between the two plates (*d*). The capacitance of a parallel-plate capacitor is defined by Equation (4):

$$C = \frac{Q}{V} = \frac{Q}{Ed} = \frac{Q}{\frac{Q}{EA}} = \frac{\varepsilon A}{d}$$
 (4)

The capacitance value is proportional to A and inversely proportional to the two conductive plate's distance, d. It is a function of the electric permittivity, ε .

2.1. Maximum Deformation of the Diaphragm

In most of the work, square, rectangular, or circular diaphragm structures are used in fabrication. Maximum deflection occurs at the centre of the diaphragm. The formula to calculate the displacement of a membrane subjected to uniform pressure loading, p, is defined in Equation (5):

$$\frac{\partial^4 w}{\partial x^4} + 2 \frac{\partial^4 w}{\partial x^2 \partial y^2} + \frac{\partial^4 w}{\partial y^4} = \frac{p}{D}$$
 (5)

In the context of a membrane, the typical displacement denoted as 'w' at a specific (x, y) coordinate corresponds to the rigidity of the membrane, represented by the symbol 'D'. This parameter is related to fundamental material properties such as Young's modulus (E), Poisson's ratio (v), and the material thickness (t), as outlined by Equation (6):

$$D = \frac{Et^3}{12(1 - v^2)} \tag{6}$$

Figure 3 illustrates the two-dimensional distribution of membrane displacement for a square membrane with fixed

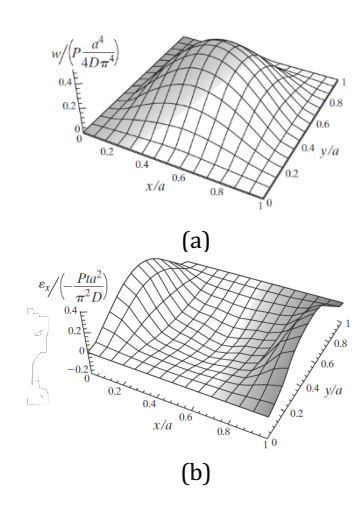


Figure 3. The visualization of normalized displacement (a) and stress occurred on the x-axis (b) [13]

boundaries, and the intensity of longitudinal stress along the x-axis. In many practical applications, only the maximum displacement and stress are of concern. These values can be estimated using an empirical formula. For a rectangular diaphragm with the dimensions of a \times b, the maximum displacement at the centre (w_center) subjected to a uniform pressure of p is determined by Equation (7):

$$w_{centre} = \frac{\alpha p b^4}{E t^3} \tag{7}$$

The value of the proportional constant α is determined by the ratio of a to b. The value of α can be found by using the look-up table in Figure 4.

2.2. Deflection of Beam

Flexural beams are commonly utilized as spring support elements in MEMS devices. The diaphragm that is attached to the flexural beams will result in higher displacement. There are multiple types of mechanical beam and their boundary condition. In this work, various sizes of two fixed and four fixed guided beams will be attached to the diaphragm to increase the maximum displacement.

The curvature of the beam under small displacement can be determined by solving a second-order differential equation of a beam, as shown in Equation (8), where E is the Young's Modulus, and I is the moment of inertia. M(x) represents the bending moment at the cross-section at location x, and y is the displacement at location x.

$$EI\frac{d^2y}{dx^2} = M(x) \tag{8}$$

By considering that the cantilever is bending in the direction of the thickness, the spring constant, k, of the beam can be calculated by using Equation (9), where w is the width, t is the thickness, and l is the length of the beam.

$$k = \frac{Ewt^3}{l^3} \tag{9}$$

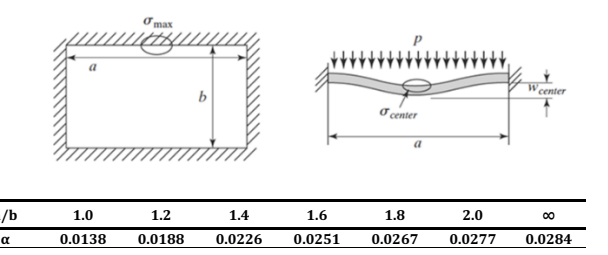


Figure 4. Bending of the rectangular plate under uniform stress [14]

2.3. Sensitivity of MEMS Capacitive Pressure Sensor

Sensitivity can be determined by using the slope of the pressure response curve, and it is an essential parameter that should be considered before choosing the right sensors. The sensitivity is defined by using Equation (10), and it gives the sensitivity unit of kPa^{-1} [15].

$$S = \frac{\Delta C}{C_o} \tag{10}$$

where S, ΔC , and C_0 are sensitivity, capacitance change, and initial capacitance of the pressure sensor, respectively. However, the sensitivity of the pressure sensor is sometimes defined by using Equation (11), and it gives the sensitivity unit of F/kPa. This work has utilized Equation (10) to determine the sensor's sensitivity.

$$S = \frac{\Delta C}{\Delta P} \tag{11}$$

3. DESIGN METHODOLOGY

The design process starts with studying the fundamentals and previous research works related to this project. Then, the sensor is designed by drawing the mask layout in the Blueprint, which is required to generate the 3D model through fabrication processes in the IntelliFab. Furthermore, the 3D models were then exported to the IntelliSuite multiphysics module ThermoElectroMechanical Analysis (TEMAnalysis). There are fundamentally three simulation settings used in this work, which are resonant frequency, static stress analysis, and static TEM relaxation.

Frequency analysis allows the user to quickly check the model setup and mesh convergence information. Since AC/frequency analyses are fast, they are often used to ensure model accuracy.

3.1. Layout Design

The design process for the MEMS capacitive pressure sensor began with creating a layout of the pressure sensor using Blueprint. The mask design consists of four layers of squares, each with the same dimensions, covering an area of 150 $\mu m \times 150~\mu m$ for the overlapped electrode. Then, this design will be imported into IntelliFab for use in the pattern transfer process. For the objective of this work, the designed layout is shown in Figure 5 (a) and (b).

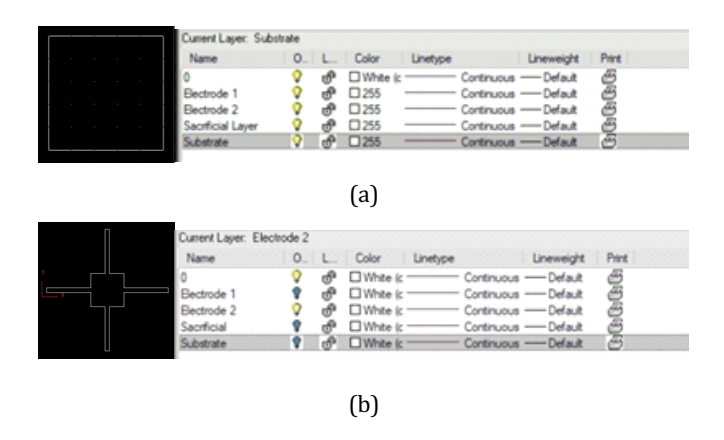


Figure 5. Mask layout in Blueprint for a MEMS capacitive pressure sensor (a) without a beam, and (b) with four beams

3.2. Microfabrication Process and 3D Model Visualization

IntelliFAB, a process simulation module within IntelliSuite, is specifically designed for the modeling and virtual fabrication of MEMS processes. It allows users to construct a detailed process flow, simulate each fabrication step, and visualize the resulting 3D structures at each stage of the process. When developing a process flow, the designer utilizes a standardized process design template and populates a process table by selecting steps such as wafer or mask definition, thin-film deposition, etching, and wafer bonding from a database containing over 70 distinct process steps. In this work, the total of 32 process steps of the fabrication process are used to create the 3D model of

the sensor. Before commencing with the procedural steps, IntelliFab needs to import the mask file from the Blueprint as part of the die setup.

In IntelliFAB, the microfabrication process is systematically defined through a series of steps. The module integrates a variety of process simulation components, encompassing deposition, etching, bonding, doping, electroplating, and liftoff, which are commonly utilized in MEMS fabrication. The process in this work consists of 32 steps, as shown in Figure 6.

After building a process flow in IntelliFab, as in Figure 6, the process flow will create a desired 3D structure. FabSim is used to view a 3D structure and cross-sections at any angle or orientation. Figure 7(a) and (b) display the 3D model visualisation and cross-sectional images of the sensors with and without the beam.

After the fabrication process in IntelliFab, the file was exported to the TEM module using Hexpresso (Isotropic Mesher) with default mesh parameters recommended by the mesh engine. This step was necessary to prepare the structure for TEM analysis. The TEM module allows for the simulation of the device's thermal, electrical, and mechanical behavior, providing insights into its performance and functionality.

In finite element analysis (FEA), a finer mesh yields more accurate results, as the smaller elements in a refined mesh are better equipped to capture stress gradients within the

Ė	F 🗹 1	ype	Material	Process	Process ID	Process Option	
	M	Definition	Si	Czochralski	Generic	,	
	V	Deposition	Mo	Bulk	Standard	Conformal Deposition	
	✓	Deposition	PR-AZ5214	Spin	001	Conformal Deposition	
	$\overline{\mathbf{A}}$	Exposure	UV	Contact	Suss		
	$\overline{\mathbf{Y}}$	Etch	Mo	Wet	Moly_Etch	Partial Etching	
	\square	Etch	PR-AZ5214	Wet	1112A	Etch Through	
	V	Deposition	SiO2	Bulk	Standard	Planarization	
	$\overline{\mathbf{v}}$	Deposition	PR-AZ5214	Spin	001	Conformal Deposition	
		Exposure	UV	Contact	Suss	·	
)	$\overline{\mathbf{v}}$	Etch	SiO2	RIE	CHF3_CF4	Etch Through	
1	$\overline{\mathbf{x}}$	Etch	PR-AZ5214	Wet	11 1 2A	Partial Etching	
2	$\overline{\mathbf{x}}$	Deposition	Mo	Bulk	Standard	Non-conformal Depositio	
3	$\overline{\mathbf{Y}}$	Deposition	PR-AZ5214	Spin	001	Conformal Deposition	
4	\square	Exposure	UV	Contact	Suss		
5	$\overline{\mathbf{v}}$	Etch	Mo	Wet	Moly_Etch	Partial Etching	
5	$\overline{\mathbf{Y}}$	Etch	PR-AZ5214	Wet	1112A	Etch Through	
7	$\overline{\mathbf{v}}$	Deposition	SiO2	LPCVD	TEOS	Planarization	
8	$\overline{\mathbf{Y}}$	Deposition	PR-AZ5214	Spin	001	Conformal Deposition	
9	1	Exposure	UV	Contact	Suss		
)	\checkmark	Etch	SiO2	RIE	CHF3_CF4	Partial Etching	
1	$\overline{\mathbf{v}}$	Etch	PR-AZ5214	Wet	11 1 2A	Partial Etching	
2	$\overline{\mathbf{x}}$	Deposition	PR-AZ5214	Spin	001	Planarization	
3	$\overline{\lor}$	Exposure	UV	Contact	Suss		
4	$\overline{\mathbf{x}}$	Etch	PR-AZ5214	Wet	1112A	Partial Etching	
5	$\overline{\mathbf{v}}$	Etch	SiO2	RIE	CHF3_CF4	Partial Etching	
5	$\overline{\mathbf{x}}$	Etch	PR-AZ5214	Wet	11 1 2A	Etch Through	
7	$\overline{\mathbf{Y}}$	Deposition	Si	PECVD	Generic	Non-conformal Deposition	
8	V	Deposition	PR-AZ5214	Spin	001	Conformal Deposition	
9	$\overline{\mathbf{x}}$	Exposure	UV	Contact	Suss		
0	V	Etch	Si	RIE	CI2_CF4	Etch Through	
1	V	Etch	PR-AZ5214	Wet	1112A	Etch Through	
2	V	Etch	SiO2	Wet	BOE	Sacrifice	

Figure 6. Microfabrication steps for a MEMS capacitive pressure sensor

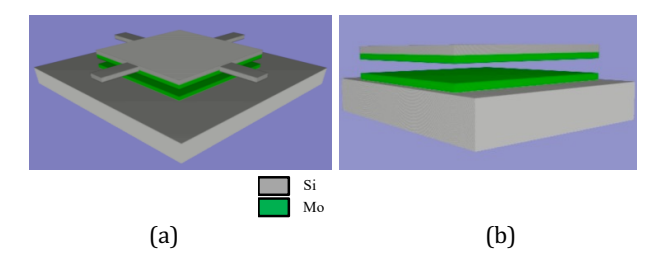


Figure 7. Mask layout in Blueprint for a MEMS capacitive pressure sensor (a) without a beam, and (b) with four beams

element. However, increasing the number of elements in a finite element model (FEM) incurs computational costs in two significant ways. First, a greater number of elements necessitates the solution of more equations at each time step, which leads to increased solution time and higher memory requirements. Second, the resultant output files from these analyses occupy more disk space for storage. Figure 8 (a) and (b) shows the imported model of TEM analysis.

After the fabrication process in IntelliFab, the file was exported to the TEM module using Hexpresso (Isotropic Mesher) with default mesh parameters recommended by the mesh engine. This step was necessary to prepare the structure for TEM analysis. The TEM module allows for the simulation of the device's thermal, electrical, and mechanical behavior, providing insights into its performance and functionality.

The subsequent step involves establishing the boundary conditions for the parallel plate. All four edges of the top electrode and the surface below the bottom electrode will be set as fixed. Then, different amounts of loads for every analysis required, such as resonant frequency, static stress analysis, and static TEM relaxation, will be applied. For static stress analysis, the value of stress/stress gradient was set from 0 to 20 MPa in increments of 2 MPa. In addition, the TEM relaxation analysis was performed by applying pressure on the top surface of the diaphragm until the displacement value reached 2 μm .

4. RESULTS AND DISCUSSION

The first result to be reported included the resonance frequency, static stress analysis, and static TEM relaxation of the capacitive sensor without a beam. Subsequently, an analysis was conducted on how varying sizes of the beams impact the sensors' performance.

4.1. The Capacitive Sensor Without Beams

A square-shaped Si diaphragm with an area of 150 μ m \times 150 μ m, a thickness of 1 μ m, separated by a 2 μ m air gap that is sandwiched by two electrodes composed of Mo with a thickness of 1 μ m each, was used in this simulation. This design has acquired the resonance frequency of 947.702 kHz, and a maximum Z-displacement of 7.88 \times 10⁻¹⁷ μ m when 20 MPa is applied in the static analysis. Figure 9 illustrates the z-displacement of the diaphragm in the z-axis when 20 MPa is applied to the structure.

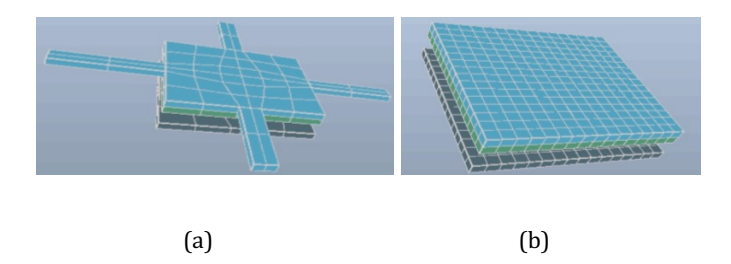


Figure 8. The 3D model visualisation and cross-sectional images of the sensors (a) with and (b) without the beam

The capacitance values attained from various pressures applied to the diaphragm's surface in this simulation are illustrated in Figure 10. The maximum capacitance value achieved is 95.89 fF at a pressure applied of 1 MPa. The design sensitivity from this design is recorded as 31.861 fF/MPa. The trend shown in the plotted graph was increasing as the pressure increased.

4.2. The Capacitive Sensor With Beams

The influence of having beams attached to the diaphragm on the sensor's performance is investigated with four different dimensions of the beams used in this work, as tabulated in Table 1.

Table 1. Four different dimensions of the beams

Width, w (μm)	Length, <i>l</i> (μm)	Thickness, t (μm)
	200	
20	150	1.0
20	100	1.0
	50	

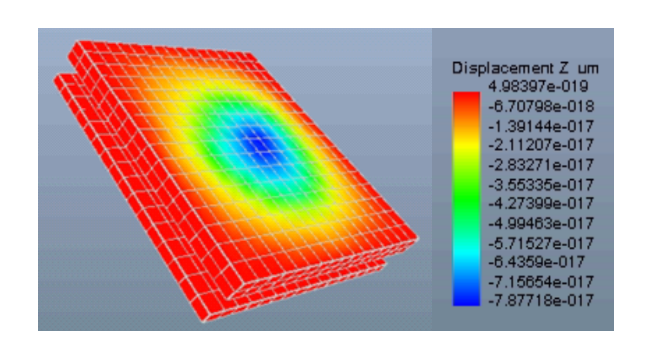


Figure 9. The Z-displacement of the diaphragm for the load of 20 MPa

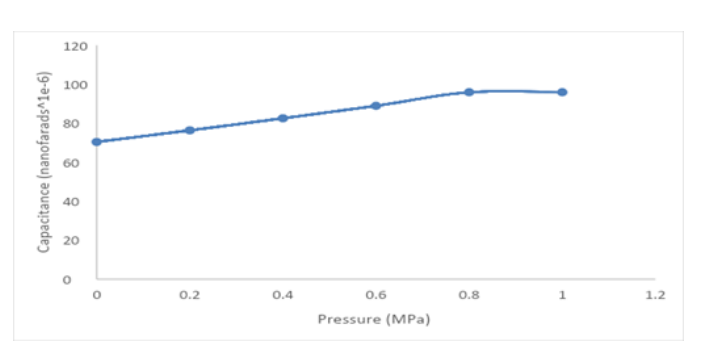


Figure 10. Capacitance value obtained with various pressures applied

Figure 11 shows the z-displacement obtained by four different dimensions of the beams with various pressures applied to the diaphragm. Analogous to the static analysis conducted on the capacitive sensor without a beam, the stress and stress gradient values were incrementally varied from 0 to 20 MPa in steps of 2 MPa. From the simulation, it was observed that the optimal performance design was obtained by a 200 μm length beam. This design has acquired the resonance frequency of 13.526 kHz, maximum Z-displacement of 0.244 μm when 20 MPa is applied in the static analysis. Figure 12 shows the distribution of Z-displacement on this optimal design for the load of 20 MPa.

In the ThermoElectroMechanical Relaxation analysis, the maximum capacitance value achieved is 1.129 pF at a pressure applied of 4 \times 10⁻⁴ MPa. This outcome corresponds to a maximum z-displacement of 2.2518 μm . Based on the simulation results, the sensitivity of this design is determined as 2.505 \times 10⁶ fF/MPa.

4.3. The Sensitivity of the MEMS Capacitive Pressure Sensor

Based on simulation results obtained in Sections 4.1 and 4.2, the sensitivity of the capacitive pressure sensor in Table 2 is calculated by using Equation (10). The highest sensitivity is $2.505\times10^6\, fF/MPa$, acquired by the sensor with a beam's dimension of 200 μm length, 20 μm width, and 1 μm thickness. In comparison to the previous work done by [12] [15], and [16], this work recorded a better performance compared to theirs.

5. CONCLUSION

The MEMS capacitive pressure sensor is designed in square-shaped Si diaphragms, attached with beams with a length of 200 μm , an overlapped area of 150 $\mu m \times 150$ μm , a thickness of 1 μm , separated by a 2 μm air gap sandwiched by two electrodes composed of Mo with a thickness of 1 μm each has resulting in the highest sensitivity among all. This capacitive pressure sensor has obtained a resonance frequency of 13.526 kHz, a maximum Z-displacement of 0.244 μm when 20 MPa pressure is applied in the static analysis, and a maximum capacitance value achieved is 1.129 pF at a pressure applied of 4 \times 10-4 MPa with sensitivity 2.505 \times 106 fF/MPa.

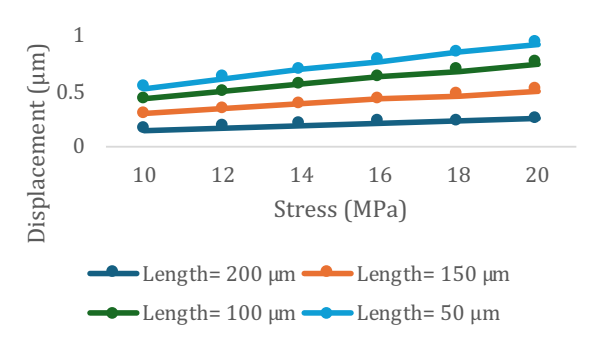


Figure 11. Z-displacement of four different dimensions of the beams with various pressures applied

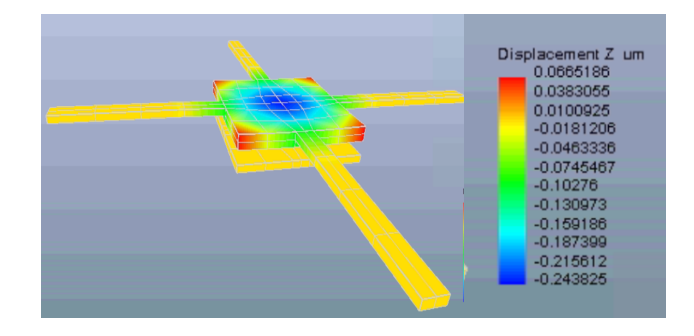


Figure 12. Distribution of Z-displacement on the diaphragm with 200 μ m length beams for the applied load of 20 MPa

ACKNOWLEDGMENTS

The author would like to thank the Faculty of Electronic Engineering & Technology, UniMAP, for providing simulation facilities used in this work, and also to acknowledge the financial support in the form of a publication incentive grant from Universiti Malaysia Perlis (UniMAP).

REFERENCES

- [1] Future Market Insights, "MEMS Pressure Sensor Market | Global Market Analysis Report 2035," 2025
- [2] Natrade, "MEMS Pressure Sensor Trends in 2025," June 2025.
- [3] J. F. Tressler, S. Alkoy, and R. E. Newnham, "Piezoelectric Sensors and Sensor Materials," *Journal of Electroceramics*, vol. 2, no. 4, pp. 257–272, 1998.

Table 2. The sensitivity of the capacitive pressure sensor

Diaphragm design	C _{min} (F)	C _{max} (F)	ΔP (MPa)	Sensitivity (fF/MPa)
Square (without beam support)	70.406 f	95.895 f	0.8	31.861
Square (4 beams attached with each beam size, $l = 200 \mu \text{m}$, $w = 20 \mu \text{m}$, and $t = 1 \mu \text{m}$)	0.108 p	1.110 p	4.0 × 10 ⁻⁴	2.505 × 10 ⁶
Square (4 beams attached with each beam size, $l=150~\mu\text{m}$, $w=20~\mu\text{m}$, and $t=1~\mu\text{m}$)	75.109 f	0.134 p	1.2 × 10 ⁻³	4.908 × 10 ⁴
Square (4 beams attached with each beam size, $l=100~\mu\text{m}$, $w=20~\mu\text{m}$, and $t=1~\mu\text{m}$)	0.107 p	0.508 p	6.0 × 10 ⁻³	66.833 × 10 ⁴
Square (4 beams attached with each beam size, $l=50~\mu \text{m}, w=20~\mu \text{m}, \text{ and } t=1~\mu \text{m})$	0.104 p	0.358 p	4.0 × 10 ⁻²	6.350 × 10 ³

- [4] P. Eswaran and S. Malarvizhi, "Design Analysis of MEMS Capacitive Differential Pressure Sensor for Aircraft Altimeter," *International Journal of Applied Physics and Mathematics*, pp. 014–020, vol. 2, no. 1, 2012.
- [5] U. S. Kumar and N. J. Babu, "Design and Simulation of MEMS Piezoresistive Pressure Sensor to Improve the Sensitivity," International Journal of Innovative Research in Electrical, Electronics, Instrumentation and Control Engineering (IJIREEICE), pp. 153–155, 2015.
- [6] M. Mousavi, M. Alzgool, and S. Towfighian, "A MEMS Pressure Sensor Using Electrostatic Levitation," *IEEE Sensors Journal*, vol. 21, no. 17, pp. 18601–18608, 2021.
- [7] C. Cui, Y. Qin, Y. Zeng, X. Lu, E. Wei, and J. Xie, "A flexible capacitive pressure sensor with dual-layer microstructure for health monitoring," *Sensors and Actuators A: Physical*, vol. 377, p. 115709, 2024.
- [8] G. R. Bi, S. K. Jindal, and S. P. Sahoo, "Investigation into electro mechanical behaviour of MEMS wing shaped dielectric capacitive pressure sensor conforming to set boundary conditions and sizing tolerances," *Scientific Reports*, vol. 15, no. 1, p. 24187, 2025.
- [9] C. Wang, "Methods to improve the sensitivity of micro-capacitive pressure sensors," *Journal of Physics: Conference Series*, vol. 2580, no. 1, p. 012050, 2023.
- [10] J. Han and M. A. Shannon, "Smooth contact capacitive

- pressure sensors in touch- and peeling-mode operation," *IEEE Sensors Journal*, vol. 9, no. 3, pp. 199–206, 2009.
- [11] R. Liang, P. Li, Y. Liu, J. Miao, J. Liao, and X. Zhuang, "Beam-membrane MEMS capacitive pressure sensor characterized with segmented comb and lever amplification mechanism," *Measurement*, vol. 250, p. 117205, 2025.
- [12] Suman and D. Bhatia, "Square Shaped MEMS Capacitive Pressure Sensors for Biological Applications," *ECS Transactions*, vol. 107, no. 1, pp. 6089–6100, 2022.
- [13] C. Liu, "Foundations of MEMS," 2nd ed. Prentice Hall Press, USA, 2011.
- [14] N. Thi Minh, "Modeling and analysic of MEMS capacitive pressure sensor using graphene membrane," *Vinh University Journal of Science*, vol. 47, no. 1A, 2018.
- [15] P. Tripathi, S. K. Pandey, and A. K. Sharma, "Design and Simulation based Analysis of Flexible Capacitive Pressure Sensor and Improvement in Sensing Characteristics," in 2021 2nd International Conference for Emerging Technology (INCET), IEEE, 2021, pp. 1–5.
- [16] Y. J. See and M. H. Ismail, "Design, Simulation and Analysis of MEMS Capacitive Pressure Sensor," in 2021 IEEE 19th Student Conference on Research and Development (SCOReD), IEEE, 2021, pp. 262–266.